

ASTROMETRIC AND PHOTOMETRIC STUDY OF THE OPEN CLUSTER NGC 2323

M. Y. Amin^{1,2} and W. H. Elsanhoury^{3,4}

¹*Astronomy Dept., Faculty of Science, Cairo University, Cairo, Egypt*

²*Physics Dept., College of Sciences and Humanities, Hawtat Sudair, Majmaah University, Saudi Arabia*

³*Astronomy Dept., National Research Institute of Astronomy and Geophysics (NRIAG),
11421, Helwan, Cairo, Egypt (Affiliation ID: 60030681)*

⁴*Physics Dept., Faculty of Science, Northern Border University, Rafha Branch, Saudi Arabia*

E-mail: welsanhoury@gmail.com

(Received: August 2, 2016; Accepted: March 2, 2017)

SUMMARY: We present a study of the open cluster NGC 2323 using astrometric and photometric data. In our study we used two methods that are able to separate open cluster's stars from those that belong to the stellar background. Our results of calculations by these two methods indicate that: 1) according to the membership probability, NGC 2323 should contain 497 stars, 2) the cluster center should be at $07^{\text{h}} 02^{\text{m}} 48^{\text{s}}.02$ and $-08^{\circ} 20' 17''.74$, 3) the limiting radius of NGC 2323 is 2.31 ± 0.04 pc, the surface number density at this radius is $98.16 \text{ stars pc}^{-2}$, 4) the magnitude function has a maximum at about $m_v = 14$ mag, 5) the total mass of NGC 2323 is estimated dynamically by using astrometric data to be $890 M_{\odot}$, and statistically by using photometric data to be $900 M_{\odot}$, and 6) the distance and age of the cluster are found to be equal to 900 ± 100 pc, and 140 ± 20 Myr, respectively. Finally the dynamical evolution parameter τ of the cluster is about 436.2.

Key words. Astrometry – Techniques: photometric – open clusters and associations: individual: NGC 2323

1. INTRODUCTION

Open clusters are important celestial objects in understanding star formation (Joshi et al. 2016). On the other hand, determination of open cluster physical parameters due to observational studies, helps us to understand the galactic structure and evolution.

The open cluster NGC 2323, or M50 or OCI-559 ($l = 221^{\circ}.7$, $b = -1^{\circ}.3$), is located nearly at the edge of CMa OB1, and was studied by several authors using photographic photometry (see, e.g. Cuffey 1941, Hoag et al. 1961, Mostafa et al. 1983, Claria et al. 1998).

This paper is structured as follows, the second section is devoted to the data used, section three gives the method of computation, section four is concerned with the results and discussion, and the section five gives the conclusion.

2. DATA

The data for cluster were taken from Frolov et al. (2012), who give the positions of stars to a limiting magnitude $B \sim 16.7$ mag. An area of 42.5×42.5 arcmin² centered on the cluster was measured on six plates from the Pulkovo normal astrograph with a maximum epoch difference of 60 yr. The measure-

ments were performed with the Pulkovo "Fantasy" automated measuring system upgraded in 2010. The corresponding areas from the USNO-A2.0 (Monet et al. 1998), USNO-B1 (Monet et al. 2003), and Two Micron All Sky Survey 2MASS database of Skrutskie et al. (2006) catalogues were used as additional plates. As a result, the relative proper motions of stars were obtained with a root-mean-square error of 5.85 mas yr^{-1} .

The total recorded number of stars from the VizieR Online Data Catalog of Frolov et al. (2012) is 1103. In our model we treat only 566 stars from this set which have no missing data of their position, proper motion, and the apparent visual magnitudes.

According to Frolov et al. (2012) all, 1103 stars are single, except for three of them, which are the well-known triple system CCDM 07030-0821, the triple system CCDM 07035-0827, and the double star CCDM 07036-0838.

Frolov et al. (2012) give the values of 9.85 mag and $\approx 1 \text{ kpc}$ for the distance modulus and distance, respectively.

3. METHOD OF COMPUTATION

In our calculations, we used the following equations and, in some cases, in combination to match our aim.

3.1. Membership probability

The criteria of multicolor photometry, and proper motion were used to define the membership in open cluster (Zhao et al. 1982). One of the main purposes of our astrometry cluster membership studies is to produce a color magnitude diagram (CMD) with reduced field-star contamination. In order to locate and discuss several features of the CMD, we set a limit to probabilities and magnitudes so as to isolate the cluster members. By this process, all cluster candidates with a probability of membership higher than 50 % and magnitudes equal to or under a threshold following from our proposed limits will be included in the CMD of the cluster.

In our calculations, we present two algorithms that are able to separate open clusters stars from those that belong to the stellar background (or foreground). In the first method, we used proper motions of individual stars based on the maximum likelihood method. While in the second method we set the probability limit to 50 % and by imposing this restriction we actually considered all-stars with probabilities less than the proposed one as the field stars. Then the field of view has been divided into strips (20-30 strips) and bins (20-30 bins) for the purpose of investigating each bin as an individual part.

For the first method: the membership probabilities in a cluster field from their proper motions, we shall consider some objective criteria for pruning the vector point diagram (VPD).

We used the method described in Sanders (1971), which assumed, for the purpose of orientation (i) a circular normal bivariate distribution function for the cluster, and (ii) an elliptical normal bivariate distribution function for the field, following Vasilevskis et al. (1957).

VPD rotation of the cluster has been done to isolate the field stars (which must remain fixed relative to the other cluster stars to get the real cluster members) using the procedure developed by (Sanders 1971) and discussed in (Zhao et al. 1982), i.e. the pruning process into which the stars are rotated in three quarters on the coordinates. By moving the stars located in the first quarter to the second and from the second to the third then to the fourth quarter and compare the resultant coordinates to the initial listed coordinates. By this rotation the field stars will be easily identified and separated and the real members will be listed (El Nazer 2014).

In what follows, we present a staggered procedure of data pruning, determinations of orientation of the field points, the distribution parameters of cluster members, and the field stars. A brief explanation of the algorithm is as follows:

1. The first pruning. Remove all stars with

$$|\mu'_{xi}| \geq 2'' \quad \text{or} \quad |\mu'_{yi}| \geq 2'', i = 1, \dots, m, \quad (1)$$

where μ'_{xi} and μ'_{yi} are proper motions of stars at x and y coordinates, respectively.

2. If m_1 are stars remain, proceed to find an approximate value of θ from the m_1 stars using

$$\mu_{ui} = \mu'_{xi} - \frac{1}{n_f} \sum_{n_f} \mu'_{xi} \quad (2)$$

$$\mu_{vi} = \mu'_{yi} - \frac{1}{n_f} \sum_{n_f} \mu'_{yi} \quad (3)$$

$$\sum_{n_f} (\mu_{vi} \cos \theta - \mu_{ui} \sin \theta)^2 = \min. \quad (4)$$

i.e.

$$\tau_g(2\theta) = \frac{2 \sum_{n_f} (\mu_{ui} \cdot \mu_{vi})}{\sum_{n_f} (\mu_{ui}^2 \cdot \mu_{vi}^2)}. \quad (5)$$

Now calculate the relative proper motion (μ_{xi}, μ_{yi}) in the rotating frame. According to Fig. 1 we have

$$\mu_{xi} = \mu'_{xi} \cos \theta + \mu'_{yi} \sin \theta$$

$$\mu_{yi} = -\mu'_{xi} \sin \theta + \mu'_{yi} \cos \theta.$$

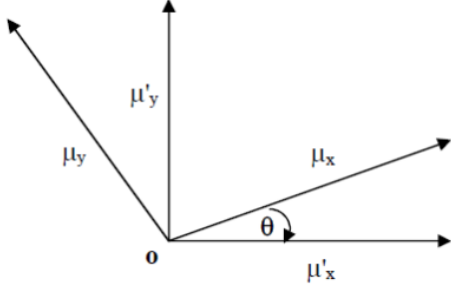


Fig. 1. *The rotating frame.*

3. The second pruning. Remove all stars with

$$|\mu'_{xi}| \geq 1.5'' \text{ or } |\mu'_{yi}| \geq 1.5'', \quad i = 1, \dots, m. \quad (6)$$

Considering: (μ_{xc}, μ_{yc}) coordinates of the cluster center in the VPD, and (μ_{xf}, μ_{yf}) coordinates of the field in the VPD. If N stars remain then solve the equations for the distribution parameters

$$\sum_{i=1}^N \left(\frac{F_A}{\sigma_x \sigma_y} - \frac{F_B}{\sigma^2} \right) = 0, \quad (7)$$

$$\sum_{i=1}^N F_A (\mu_{xi} - \mu_{xf}) = 0, \quad (8)$$

$$\sum_{i=1}^N F_A (\mu_{yi} - \mu_{yf}) = 0, \quad (9)$$

$$\sum_{i=1}^N F_B (\mu_{xi} - \mu_{xc}) = 0, \quad (10)$$

$$\sum_{i=1}^N F_B (\mu_{yi} - \mu_{yc}) = 0, \quad (11)$$

$$\sum_{i=1}^N F_A \left[\left(\frac{\mu_{xi} - \mu_{xf}}{\sigma_x} \right)^2 - 1 \right] = 0, \quad (12)$$

$$\sum_{i=1}^N F_A \left[\left(\frac{\mu_{yi} - \mu_{yf}}{\sigma_y} \right)^2 - 1 \right] = 0, \quad (13)$$

$$\sum_{i=1}^N F_B \left[\left(\frac{\mu_{xi} - \mu_{xc}}{\sigma} \right)^2 + \left(\frac{\mu_{yi} - \mu_{yc}}{\sigma} \right)^2 - 2 \right] = 0, \quad (14)$$

in which:

$$F_B = F_A F, \quad (15)$$

$$F_A = 2n \left(\frac{1 - n^2}{\sigma_x \sigma_y} + \frac{n_c}{\sigma^2} F \right)^{-1},$$

$$F = \exp \left\{ \frac{1}{2} \left[\left(\frac{\mu_{xi} - \mu_{xf}}{\sigma_x} \right)^2 + \left(\frac{\mu_{yi} - \mu_{yf}}{\sigma_y} \right)^2 - \left(\frac{\mu_{xi} - \mu_{xc}}{\sigma} \right)^2 - \left(\frac{\mu_{yi} - \mu_{yc}}{\sigma} \right)^2 \right] \right\}. \quad (16)$$

Calculate the membership probabilities:

$$P_i = \frac{F_B n_c}{2\pi\sigma^2}, \quad (17)$$

identify individual members and field stars based on the membership probabilities, and the total number n_c of members. Calculate once again the angle from the field stars that are obtained and the rotated proper motions, i.e. repeat steps (2) and (3).

4. The third pruning. Remove all stars with:

$$\mu_{xi} \leq \mu_{xf} - 2\sigma_x \quad \text{and} \quad \mu_{xi} \geq \mu_{xf} + 2\sigma_x$$

$$\mu_{yi} \leq \mu_{yf} - 2\sigma_y \quad \text{and} \quad \mu_{yi} \geq \mu_{yf} + 2\sigma_y.$$

5. If N_1 stars remain, repeat steps (5) and (6) with N_1 stars and find the final values of the distribution parameters and the membership probabilities.

3.2. Field stars density

To calculate the field stars density (Ismail and Marie 2001), we separated the cluster members from the total number of the cluster stars and then divided the resultant number by the area of the field around the cluster

$$d_f = \frac{N_f}{A_f} \pm \frac{\sqrt{N_f}}{A_f},$$

where:

N_f is the number of field stars,
 A_f is the area of the field region.

3.3. Density in strips

We divided the plate into many vertical and horizontal strips of equal widths and then counted the number of stars in each bin relative to its boundaries of horizontal and vertical coordinates.

The density distribution in right ascension is defined by

$$D\alpha_{(J-1)} = \frac{M\alpha_{(J-1)} \times NST}{(\alpha_{\max} - \alpha_{\min}) \times (\delta_{\max} - \delta_{\min})}. \quad (18)$$

While, the density distribution in declination is defined by

$$D\delta_{(J-1)} = \frac{M\delta_{(J-1)} \times NST}{(\delta_{\max} - \delta_{\min}) \times (\alpha_{\max} - \alpha_{\min})}, \quad (19)$$

where:

J	is the strip number,
NST	is the number of strips,
$\alpha_{(J-1)}$	is the right ascension of strip at $(J-1)$,
$\delta_{(J-1)}$	is the declination of strip at $(J-1)$,
α_{\max} & α_{\min}	is max. and min. right ascension,
δ_{\max} & δ_{\min}	is max. and min. declination.

3.4. Stellar density distribution

We find the density of stars in rings along a projected radius (at any distance) from the core to the maximum distance from the center (max. radius).

The problem of the space distribution of stars in the cluster has been noted by many investigators of whom we mention Leonard et al. (1992), Amin et al. (1997) and Balaguer-Núñez et al. (1998). The density distribution was determined using the same technique as described by Amin et al. (1997) and checked by the method used in Balaguer-Núñez et al. (1998). The surface density distribution takes the form:

$$\rho(R) = \rho_0 \left[1 + (R/r_0)^2 \right]^{-2}, \quad (20)$$

where:

ρ_0	is surface density at the center,
R	is projected radius,
r_0	is core radius.

In this method, the counting stars brighter than the completeness limit was obtained in two orthogonal rectangular strips. The strips were aligned with right ascension and declination; these strips were divided into 30 bins along their lengths.

When plotting the density of the bins versus the position along the strip, the center of symmetry about the peak will be taken to be the cluster center, and the projected density distribution will be calculated by counting the star distributed in rings around the center (Marie and Ismail 2002).

3.5. Mass estimation

To estimate the dynamical mass (Amin et al. 1997) in the region of the stellar systems from the stellar hydrodynamics, we must solve the Jeans equation using the proper motion data, employing the same technique as used by Leonard et al. (1992). By this technique we simply get the first velocity moment of the collisionless Boltzmann equation in which the acceleration is replaced by the gradient of the gravitational potential. For a spherical stellar system that is not (or is only slowly) rotating, the Jeans equation becomes

$$GM(r) = -\frac{r^2}{n} \frac{d(n\sigma_r^2)}{dr} - 2r(\sigma_r^2 - \sigma_t^2), \quad (21)$$

where G is the gravitational constant, $M(r)$ is the mass of all matter in the system inside the spherical shell of radius r centered in the system, where

$n(r)$, $\sigma_r(r)$ and $\sigma_t(r)$ are, respectively, the density of tracer population in the system and the velocity dispersion of the tracers as a function of radius parallel and tangential (in one dimension) to the radius vector in the system; $n(r)$, $\sigma_r(r)$ and $\sigma_t(r)$ correspond only to some homogeneous population of tracer objects which may or may not contribute significantly to the total mass of the system. In our model $n(r)$ is given by

$$n(r) = n_0 \left[1 + (r/r_0)^2 \right]^{-5/2}, \quad (22)$$

where n_0 is the density at the center.

For estimating the dynamical mass in the region of the stellar systems from the stellar hydrodynamics, we must solve the Jeans equation using the proper motion data, using the same technique as Leonard et al. (1992).

Following Leonard et al. (1992), in our model the quantities $\sigma_r(r)$ and $\sigma_t(r)$ are given by:

$$\sigma_r(r) = \sigma_0 [\sigma_{\text{iso}}(r) / \sigma_0]^{n_r}, \quad (23)$$

and

$$\sigma_t(r) = \sigma_0 [\sigma_{\text{iso}}(r) / \sigma_0]^{n_t}, \quad (24)$$

where σ_0 is the central velocity dispersion and $\sigma_{\text{iso}}(r)$ is the isotropic velocity dispersion profile given by

$$\sigma_{\text{iso}}(r) = \sigma_0 \left[1 + (r/r_0)^2 \right]^{-1/4}. \quad (25)$$

4. RESULTS AND DISCUSSION

In our study we obtain physical parameters of the cluster by using astrometry and photometry methods. In our calculations we used the data of Frolov et al. (2012), which only used photometric analysis to obtain the parameters of NGC 2323 in their study. Before the calculations of astrometric and photometric parameters of NGC 2323 we should check the membership of stars in the cluster, because these parameters depend on membership, except the coordinates of the cluster's center.

In the beginning of our calculations of membership we used a data file containing 566 out of 1103 field stars for NGC 2323 which has no missing data of their position, proper motion, and the apparent visual magnitudes. Our data on 566 stars only contained one triple system CCDM 07030–0821 which we assumed as a single star, the other two systems are neglected in our calculations due to the triple system CCDM 07036–0838 has not a complete data, and the double system CCDM 07035–0827 has a probability of 25%.

Our calculation of membership stars for the NGC 2323 cluster by using two methods indicates that:

1. The membership by the first method (Sander's methods) which depends on relative proper motions of clusters (i.e. the first, second, and third pruning with angle of rotation) are 497 stars as given in Table 1.

Table 1: The results of the first, second, and third pruning

Pruning	No. of cancelled stars	No. of membership stars	Angle of rotation (θ)
First	36	530	90°545
Second	33	497	45°734
Third	0	497	0°642

Table 2: The distribution of membership stars in the cluster

Bin No.	Radius (R_{pc})	No. of membership stars	Density (No. of membership stars/area)
1	2.22	210	13.5632
2	2.238	5	19.4966
3	2.257	1	3.8676
4	2.275	11	42.1994
5	2.293	16	60.8889
6	2.312	26	98.1577
7	2.33	9	33.7094
8	2.348	15	55.743
9	2.366	16	58.997
10	2.385	12	43.9068
11	2.403	12	43.5708
12	2.421	10	36.0336
13	2.44	8	28.6096
14	2.458	18	63.8907
15	2.476	17	59.8931
16	2.495	14	48.9602
17	2.513	12	41.6592
18	2.531	8	27.5712
19	2.55	9	30.7939
20	2.568	1	3.3971

Note: We find the density of stars in rings along a projected radius (at any distance) from the core to the maximum distance from the center (max. radius).

2. The memberships by the second method, as mentioned before, are 497 stars too. Table 2 shows the number of membership stars in each bin. From this table we noticed that most of the membership stars are located at the center of the cluster.

Therefore our two methods of calculation are in agreement with each other. Consequently, the other calculated parameters for the NGC 2323 cluster will be done for those members (i.e. 497 stars).

By analyzing these data, we found that:

- (i) The maximum and minimum α are $07^{\text{h}} 03^{\text{m}} 54^{\text{s}}86$, and $07^{\text{h}} 01^{\text{m}} 34^{\text{s}}46$, respectively.
- (ii) The maximum and minimum δ are $-08^{\circ} 04' 0''52$, and $-08^{\circ} 36' 58''$, respectively.
- (iii) The faintest and brightest apparent magnitudes in infrared band are 16.82 mag and 7.86 mag; while for Frolov et al. (2012) they are 15.6 mag and 7.86 mag, respectively. This is due to the difference of membership in our model and Frolov et al. (2012).
- (iv) Our estimated mass is about $890 M_{\odot}$ while for Frolov et al. (2012) it is within the range ($870 \leq M_{\odot} \leq 1305$).

From our results in Table 1 we noticed that the number of membership stars is 497 while the number of

member stars according to Frolov et al. (2012) is 508.

4.1. Astrometric parameters

The data of the NGC 2323 cluster was taken from Frolov et al. (2012) with the total recorded number of 1103 stars. In our calculations, we used the distance modulus equal to 9.85 mag and the membership equal to 497 stars.

4.1.1. Cluster's center determination

We started the data analysis by re-determining the cluster center, using the common procedure presented by many authors e.g. Maciejewski and Niedzielski (2007), Maciejewski et al. (2009), and Haroon et al. (2014). In this procedure, two perpendicular strips were cut along the right ascension and declination at an approximate center of the cluster, and then the histograms of the star counts have been built along each strip. The histograms of both coordinates are fitted by a Gaussian distribution function; its maximum value gives the position

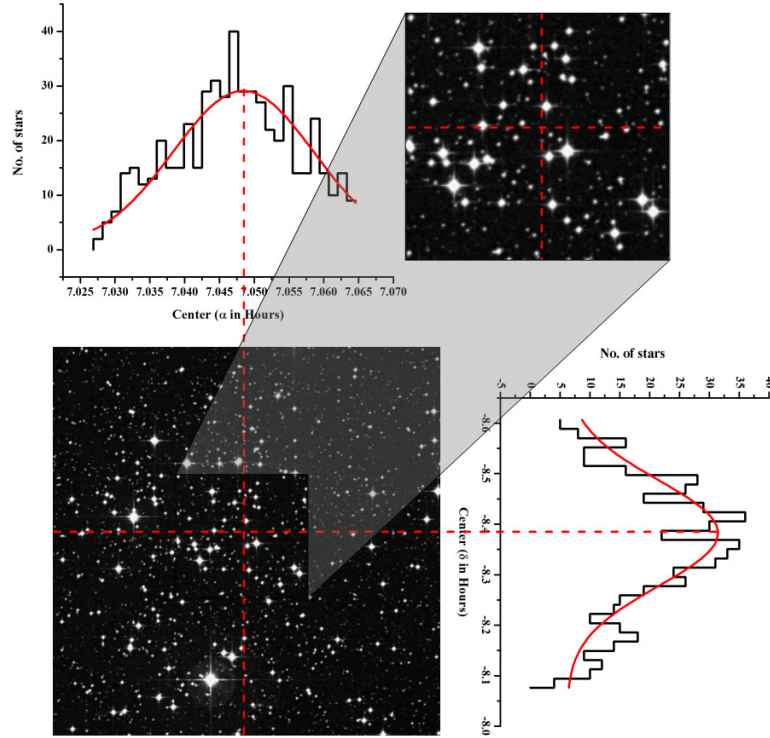


Fig. 2. The Gaussian fit provides the coordinates of highest density areas in α and δ on NGC 2323 ($\alpha = 07^{\text{h}} 02^{\text{m}} 48^{\text{s}}.02$, $\delta = -08^{\circ} 20' 17''.74$), and ($l = 221^{\circ}.644$, $b = -1^{\circ}.2887$).

of the new cluster center for 1103 stars, as shown in Fig. 2. From this figure, we get that the equatorial coordinates ($\alpha = 07^{\text{h}} 02^{\text{m}} 48^{\text{s}}.02$, and $\delta = -08^{\circ} 20' 17''.74$) and galactic coordinates ($l = 221^{\circ}.644$ and $b = -1^{\circ}.2887$) for the NGC 2323 open cluster.

By comparing our calculated results with Frolov et al. (2012), we noticed that the calculated right ascension and the declination are both greater than that given by Frolov et al. (2012) by about $0^{\text{s}}.52$ and $1''.74$, respectively.

4.1.2. Apparent magnitude function

Fig. 3 represents our calculations of the apparent magnitude function of NGC 2323.

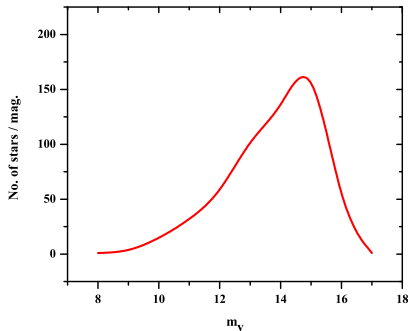


Fig. 3. The apparent magnitude function of NGC 2323.

As seen from the figure, this function has a maximum at about $m_v = 14$ mag corresponding to 162 stars per mag. This result is the first one for magnitude functions for NGC 2323.

4.1.3. Density distribution of stars

Our calculated results for the radial density profile (i.e. distribution) of stars corresponding to limiting radius of bins during the cluster are shown in Table 2 and Fig. 4. From this distribution curve we notice that: the distribution of stars inside the cluster radius equal to 2.22 pc is practically straight, and the maximum density value is $98.16 \text{ stars pc}^{-2}$ produced by 26 stars located at limiting radius r_{lim} from the center. Our calculated result $r_{\text{lim}} = 8.9 \pm 0.15$ arcmin (2.31 ± 0.04 pc) is less than that of Frolov et al. (2012) by about 0.31 pc. This discrepancy is due to our calculation of membership (i.e the difference in heliocentric distances between our model (900 ± 100 pc) and Frolov et al. (2012) model ≈ 1 kpc). The surface density in Fig. 4 approximately follows the law given by Eq. (20) with $r_0 = 0.104$ pc.

4.1.4. Dynamical mass

By using proper motion data and applying Eqs. (21) and (22) we infer an isotropic velocity distribution given by Eq. (25) with $\sigma_0 = 4.3659 \text{ km/s}$. Then using the well-known expression:

$$\sigma_0^2 = \frac{1}{2} \frac{GM}{r_0}$$

We obtain that the total mass of the open cluster NGC 2323 is $890 M_{\odot}$ ($r_0 = 0.104$ pc, as given above). This value is in the range of mass estimated by Frolov et al. (2012), i.e. ($870 \leq M_{\odot} \leq 1305$).

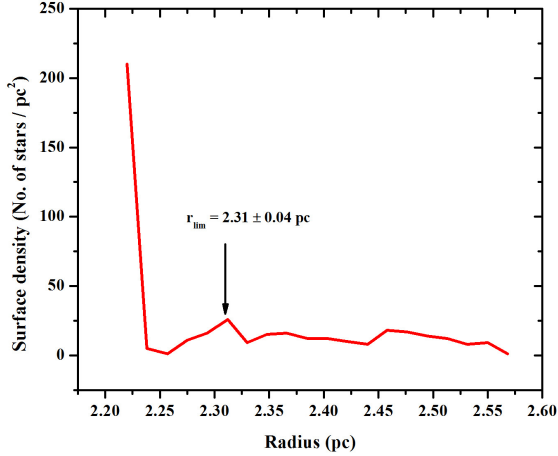


Fig. 4. The density distribution of stars in cluster.

4.1.5. Contour map

To investigate the existence of any dark matter or other star clusters near the cluster under investigation, we draw the contour map of the stellar density of the NGC 2323 region. The contour map was generated from a 400×400 density grid centered on the cluster. The density at each grid point was calculated from the number of stars brighter than the completeness limit with 2 arcmin radius, the spacing of the grid points was 2 arcmin too. The resulting contour map is shown in Fig. 5, the field star density around the cluster fluctuating, and there appear to have obvious dark clouds or other star clusters in the region.

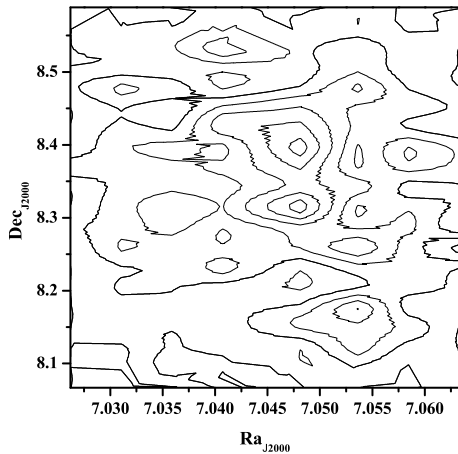


Fig. 5. The contour map of NGC 2323.

4.2. Photometric parameters

4.2.1. Color magnitude diagram CMD

Many of photometric parameters of NGC 2323 open cluster (e.g. age, reddening and distance, etc.), could be found through CMDs in three near-infrared bands J, H, and K_s . By fitting several theoretical Padova isochrones¹, Bonatto et al. (2004) of different ages, an excellent fits to CMD of $\log T_{\text{age}} = 8.15 \pm 0.05$ and solar metallicity equal to 0.019, could be presented in Fig. 6.

As we know, the reddening determination is one of the major steps in cluster compilation, guided by Schlegel et al. (1998), and Schlafly and Finkbeiner (2011). Therefore, to calculate the color excess transformations, we used the coefficient ratios $A_J/A_V = 0.276$ and $A_H/A_V = 0.176$ which are given by Schlegel et al. (1998) while the ratio $A_{K_s}/A_V = 0.118$ was derived from Dutra et al. (2002) by applying the calculations of Fiorucci and Munari (2003) for the color excess of 2MASS photometric system, i.e. $E(J-H)/E(B-V) = 0.309 \pm 0.130$, and $E(J-K_s)/E(B-V) = 0.485 \pm 0.150$, where $R_V = A_V/E(B-V) = 3.1$.

By using the last relations to correct the effects of reddening in CMDs with extinction coefficient equal to 0.992 mag for NGC 2323 open cluster, we obtained $A_{K_s}/E(B-V) = 0.366$, $A_J/E(B-V) = 0.856$. Our obtained value of reddening is greater than that obtained by Frolov et al. (2012) by about 0.07.

Our results for CMD of NGC 2323 indicate that:

1. After taking into account the effect of extinction coefficients in our calculations, we have found that the distance modulus ($m_v - M_v$) equals to 10.75 mag which is greater by about 0.9 than the result of Frolov et al. (2012).
2. From our calculations, we have the cluster apparent magnitude $m_v = 12.83$ while the cluster absolute magnitude is $M_v = 2.08$ mag.
3. Our calculation indicates that the cluster distance equals to 900 ± 100 pc [$(1.852 \pm 0.206) \times 10^{-5}$ arcmin] while in Frolov et al. (2012) it is about 1 kpc.
4. Due to our calculations, we have the cluster age T_{age} of about 140 ± 20 Myr while in Frolov et al. (2012) it is about 140 Myr.
5. $E(J-K_s) = 0.155$, and $E(J-H) = 0.099$.

On the other hand, the cluster-Sun distance is used to determine the cluster's distance to the galactic center R_{gc} , and the projected distances on the galactic planes X_{\odot} and Y_{\odot} , and the distance from the galactic plane Z_{\odot} . Our calculations of R_{gc} , X_{\odot} , Y_{\odot} , and Z_{\odot} based on Tadross (2012) are represented by 8547 pc, -667 pc, -594 pc, and -20 pc, respectively.

¹<http://stev.oapd.inaf.it/cgi-bin/cmd>

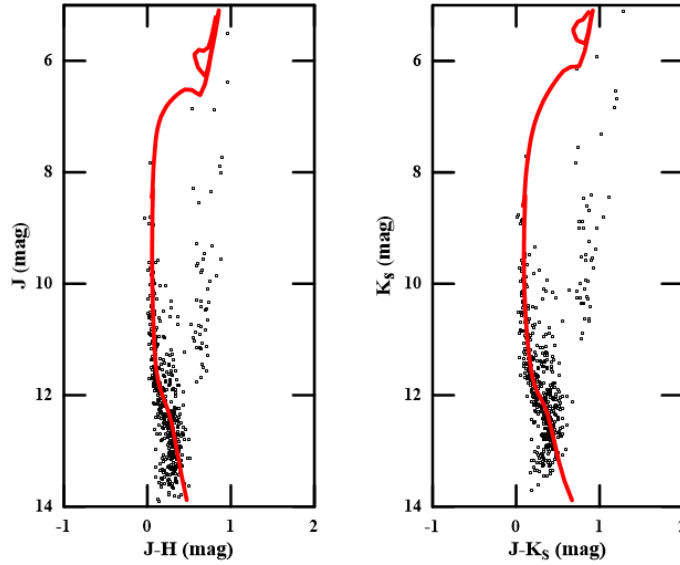


Fig. 6. Padova solar like stars (metallicity = 0.019) isochrones with $\log T_{\text{age}} = 8.15 \pm 0.05$ is drawn for CMDs of the NGC 2323 open cluster.

4.2.2. Luminosity and mass functions

The stellar luminosity function (LF) is used to study the properties of large groups or classes of objects (e.g. stars in clusters or the galaxies in the Local Group). For our purpose, the LF is defined as the total number of stars in a certain absolute magnitude. Fig. 7 shows the frequency distributions of absolute magnitudes using a bin size of 0.5.

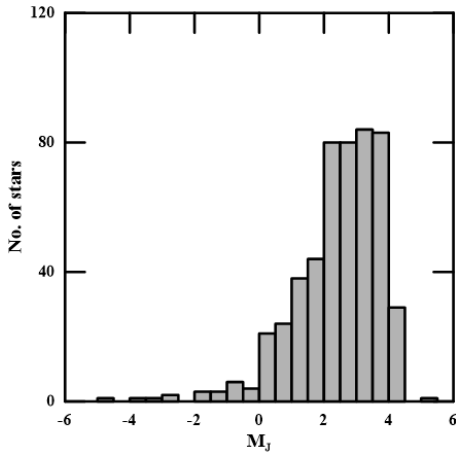


Fig. 7. The apparent LF of NGC 2323 open cluster under consideration.

The LF and mass function (MF) are correlated to each other according to the mass-luminosity relation (MLR). The field contamination of the cluster members, the observed incompleteness at low-luminosity (or low-mass) stars, mass segregation and accurate determination of the initial mass function (IMF) prevent accurate determination of both the LF and the MF, which may affect even poorly pop-

ulated, relatively young clusters (Scalo 1986). The IMF is an empirical relation that describes the mass distribution (a histogram of stellar masses) of a population of stars in terms of their theoretical initial mass (the mass they were formed with). The IMF is defined in terms of a power law as follows:

$$\frac{dN}{dM} \propto M^{-\Gamma}, \quad (26)$$

where, dN/dM is the number of stars in mass interval $(M, M + dM)$, and Γ is a dimensionless exponent.

From Salpeter (1955), the IMF for massive stars ($> 1M_{\odot}$) has been studied and well established (i.e. $\Gamma = 2.35$). The steep slope of the IMF indicates that the number of the low-mass stars is greater than that of the high-mass ones. MLR of this open cluster could be constructed here due to adopted isochrones (Bonatto et al. 2004), the relation is a polynomial function of second order, as shown in Fig. 8, i.e.

$$M/M_{\odot} = 2.840 - 0.591 \times M_{K_s} + 0.0339 \times M_{K_s}^2 \quad (27)$$

Our calculations of MF for the NGC 2323 open cluster is shown in Fig. 9, and from this figure we can obtain the slope of this function to be 3.26 ± 0.14 . By comparing our result with Salpeter (1955) a very good agreement is achieved. Also, this result is greater by about 0.07 than that of Frolov et al. (2012).

Estimation of the total mass of the cluster NGC 2323, based on Eq. (27) gives us the total mass of about $900 M_{\odot}$. By comparing this value with that of Frolov et al. (2012), we notice that our calculated value is within the range of their work (i.e. $870 \leq M_{\odot} \leq 1305$). Also our model indicates that the lower mass limit is about $0.794 M_{\odot}$, the upper mass limit is about $7.077 M_{\odot}$, and the average mass is about $1.783 M_{\odot}$.

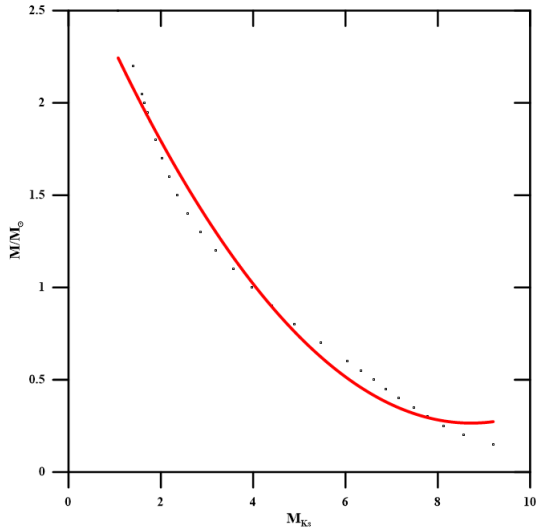


Fig. 8. Relation between the magnitude M_{K_s} and mass M/M_{\odot} from isochrones (Bonato et al. 2004) of metallicity equal to 0.019 for NGC 2323.

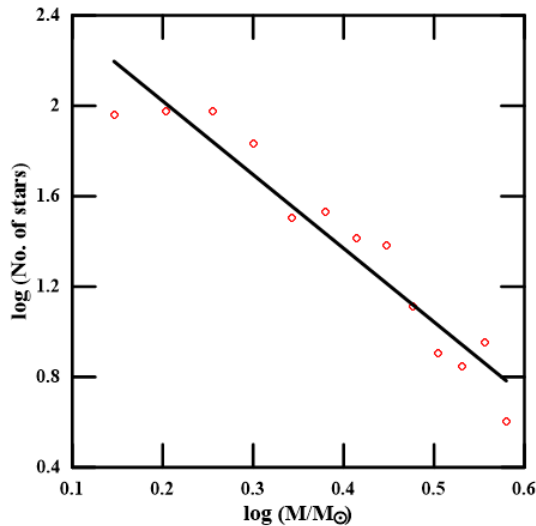


Fig. 9. Mass functions of the NGC 2323 open cluster with slope of -3.26 ± 0.14 .

Since Kroupa (2001) model gives that for any open cluster of one to four solar masses the average mass equals to $1.55 M_{\odot}$, therefore, by comparing the results of our model with that of Kroupa (2001), we get our average mass to be greater by $0.232 M_{\odot}$.

By using our total mass estimation and the relation (28), which is given by Jeffries et al. (2001), our result gives a tidal radius r_t of about 14.78 pc, i.e.

$$r_t = 1.46 \sqrt[3]{M_c}. \quad (28)$$

4.2.3. Dynamical state

The relaxation time T_{relax} of a cluster is defined as the time in which the stellar velocity distri-

bution becomes Maxwellian. Through the dynamical relaxation time, the low mass stars in a cluster may possess the largest random velocities trying to occupy a larger volume than the high mass stars do (Mathieu and Latham 1986). Mathematically, relaxation time has the form (Spitzer and Hart 1971)

$$T_{\text{relax}} = \frac{8.9 \times 10^5 \sqrt{N} R_h^{3/2}}{\langle M \rangle^{1/2} \log(0.4N)}. \quad (29)$$

The half-mass radius R_h is about $1.3 r_o$, N is the number of cluster members and $\langle M \rangle$ is the average mass of the cluster stars. Our calculations for these parameters are represented by 0.14 pc, 497 stars, and $1.782 M_{\odot}$, respectively.

Also, by using Eq. (29), we can estimate the dynamical relaxation time of the NGC 2323 open cluster T_{relax} to be about 0.321 Myr.

By using our calculated cluster age $T_{\text{age}} = 140 \pm 20$ Myr, and our calculated value of the dynamical relaxation time $T_{\text{relax}} = 0.321$ Myr, we have obtained the dynamical evolution parameter

$$\tau = \frac{T_{\text{age}}}{T_{\text{relax}}} \quad (30)$$

of the cluster to be about 436.2. Consequently, the cluster NGC 2323 can be considered dynamically relaxed.

5. CONCLUSION

The main aim of our study is to obtain the physical parameters of the cluster by using astrometry and photometry methods. In our calculations we used the data of Frolov et al. (2012), who only used photometric analysis to obtain the parameters of NGC 2323 in their study.

Our calculated results are summarized as the following points:

- We have determined the membership probability by means of the maximum likelihood method and the method of probability limit 50%. Our results of calculations by the two methods indicate that the membership probability for NGC 2323 is 497 stars while the number of member stars according to Frolov et al. (2012) is 508.
- The density distribution of right ascension and declination, is showing a small difference ($0^{\text{s}}52$ and $1^{\text{m}}74$, respectively) from that of the Frolov et al. (2012).
- Our study of NGC 2323 is the first one to compute the magnitude function of that cluster and has a maximum at about 14 mag, which is corresponding to 162 stars.
- From studying the structure of the cluster, our limiting radius is less than that of Frolov et al. (2012) by about 0.31 pc.
- Construction of CMD of Solar metallicity equal to 0.019, allows us to calculate some of the photometric parameters of NGC 2323 like the distance modulus $(m_v - M_v) = 10.75$ mag, the reddening $E(B-V) =$

0.32, and the age T_{age} of about $= 140 \pm 20$ Myr. This values are greater (slightly) than those obtained by Frolov et al. (2012). While the values of $E(\text{J-Ks}) = 0.155$, $E(\text{J-H}) = 0.099$ were not calculated by Frolov et al. (2012).

- The LF and MF are determined by applying the corrections of data field star contamination. The LF showed a gradual increase towards the low luminosity stars from the high luminosity ones. On the other hand, the value of the MF slope was about -3.26 ± 0.14 which was found to be around the Salpeter's value as shown in Fig. 9.

- In mass estimation, we used two methods, first of them followed by the Jeans equation, and the second by MF, and the results are $890 M_{\odot}$ and $900 M_{\odot}$, respectively, which is in the range deduced by Frolov et al. (2012), (i.e. $870 \leq M_{\odot} \leq 1305$).

- The cluster may be regarded as dynamically relaxed and the mass segregation effect due to dynamical evolution must be considered as an important factor.

Acknowledgements – This publication makes use of data products from the Two Micron All Sky Survey, which is a joint project of the University of Massachusetts and the Infrared Processing and Analysis Center/California Institute of Technology, funded by the National Aeronautics and Space Administration (NASA) and the National Science Foundation (NSF).

REFERENCES

- Amin, M. Y., Rassem, M. and Marie, M.: 1997, *Astrophys. Space Sci.*, **250**(1), 137.
- Balaguer-Núñez, L., Nezhinskij, K. P. and Zhao, J. L.: 1998, *Astron. Astrophys.*, **133**, 387.
- Bonatto, Ch., Bica, E. and Girardi, L.: 2004, *Astron. Astrophys.*, **415**, 571.
- Claria, J. J., Piatti, A. E. and Lapasset, E.: 1998, *Astro. Astrophys. Suppl.*, **128**, 131.
- Cuffey, J.: 1941, *Astrophys. J.*, **94**, 55.
- Dutra, C. M., Santiago, B. X. and Bica, E.: 2002, *Astron. Astrophys.*, **381**, 219.
- El Nazer, M.: 2014, M. Sc. Thesis, Cairo University.
- Fiorucci, M. and Munari, U.: 2003, *Astron. Astrophys.*, **401**, 781.
- Frolov, V. N., Ananjevskaja, Yu. K. and Polyakov, E. V.: 2012, *Astron. Lett.*, **38**(2), 74.
- Haroon, A. A., Ismail, H. A. and Alnagahy, F. Y.: 2014, *Astrophys. Space Sci.*, **352**, 665.
- Hoag, A. A., Johnson, H. L., Iriarte, B., et al.: 1961, *Publ. U. S. Naval Obs.*, **17**, 343.
- Ismail, M. N., and Marie, M.: 2001, *Al-Azhar Bulletin of Science*, **1**, 637.
- Jeffries, R. D., Thurston, M. R. and Hambly, N. C.: 2001, *Astron. Astrophys.*, **375**, 863.
- Joshi, Y. C., Dambis, A. K., Pandey, A. K. and Joshi, S.: 2016, arXiv:1606.06425v1.
- Kroupa, P.: 2001, *Publ. Astron. Soc. Pac.*, **228**, 187.
- Leonard, P. J. T., Richer, H. B. and Fahlman, G. G., 1992, *Astron. J.*, **104**(6), 2104.
- Maciejewski, G. and Niedzielski, A.: 2007, *Astron. Astrophys.*, **467**, 1065.
- Maciejewski, G., Mihov, B. and Georgiev, Ts.: 2009, *Astron. Nachr.*, **330**, 851.
- Marie, M. and Ismail, M. N.: 2002, *New Astron.*, **7**, 101.
- Mathieu, R. D. and Latham, D. W.: 1986, *Astron. J.*, **92**, 1364.
- Mostafa, A. A., Hassan, S. M., Aiad, A. and Ahmed, T.: 1983, *Astron. Soc. of Egypt*, **5**, 23.
- Monet, D. et al.: 1998, A Catalog of Astrometric Standards, U. S. Naval Obs. Flagstaff Station (USNOFS) and Universities Space Research Association (USRA) stationed at USNOFS.
- Monet, D. G., Levine, S. E., Canzian, B., Ables, H. D., Bird, A. R., Dahn, C. C., et al., 2003, *Astron. J.*, **125**(2), 984.
- Salpeter, E. E.: 1955, *Astrophys. J.*, **121**, 161.
- Sanders, W.: 1971, *Astron. Astrophys.*, **14**, 226.
- Spitzer, L. and Hart, M. H.: 1971, *Astrophys. J.*, **166**, 483.
- Scalo, J. M.: 1986, *Fundamentals of Cosmic Physics*, **11**, 1.
- Schlegel, D. J., Finkbeiner, D. P. and Davis, M.: 1998, *Astron. J.*, **500**(2), 525.
- Skrutskie, M. F., Cutri, R. M., Stiening, R., Weinberg, M. D., Schneider, S., Carpenter, J. M., et al.: 2006, *Astron. J.*, **131**, 1163.
- Schlafly, E. F. and Finkbeiner, D. P.: 2011, *Astron. J.*, **737**(2), 103.
- Tadross, A. L.: 2012, *Research in Astron. Astrophys.*, **12**(2), 158.
- Vasilevskis, S. and Rach, R. A.: 1957, *Astron. J.*, **62**, 175.
- Zhao, Y-L., Tian, K-P., Xu, Z-H. and Yin, M-G.: 1982, *Chin. Astron. Astrophys.*, **6**, 293.

**АСТРОМЕТРИЈСКА И ФОТОМЕТРИЈСКА СТУДИЈА
РАЗВЕЈАНОГ ЈАТА NGC 2323**

M. Y. Amin^{1,2} and W. H. Elsanhoury^{3,4}

¹*Astronomy Dept., Faculty of Science, Cairo University, Cairo, Egypt*

²*Physics Dept., College of Sciences and Humanities, Hawtat Sudair, Majmaah University, Saudi Arabia*

³*Astronomy Dept., National Research Institute of Astronomy and Geophysics (NRIAG),
11421, Helwan, Cairo, Egypt (Affiliation ID: 60030681)*

⁴*Physics Dept., Faculty of Science, Northern Border University, Rafha Branch, Saudi Arabia*

E-mail: welsanhoury@gmail.com

УДК 524.45 NGC2323

Стручни чланак

Представљамо студију развејаног јата NGC 2323 спроведену коришћењем астрометријских и фотометријских података. У нашој студији примењена су две методе које могу да раздвоје звезде из развејаног јата од оних из звездане позадине. Резултати наших израчунавања помоћу ова два метода указују да: 1) према вероватноћи за припадност јату NGC 2323 би требало да садржи 497 звезда, 2) центар јата би требало да се налази на $07^{\text{h}} 02^{\text{m}} 48^{\text{s}}.02$ и $-08^{\circ} 20' 17''.74$, 3) гранични

радијус за NGC 2323 је 2.31 ± 0.04 pc, а површинска густина звезда на овом радијусу је 98.16 звезда pc^{-2} , 4) функција магнитуде има максимум на око $m_v = 14$ mag, 5) укупна маса NGC 2323 процењена је динамички коришћењем астрометријских података на $890 M_{\odot}$, и статистички коришћењем фотометријских података на $900 M_{\odot}$, и 6) нађено је да су удаљеност и старост јата 900 ± 100 pc, и 140 ± 20 Myr, тим редом. Напошетку, параметар динамичке еволуције јата τ износи око 436.2.